Stereoselective ROP of *rac*-Lactide Mediated by Enantiopure NNO-Scorpionate Zinc Initiators.

Manuel Honrado,[†] Antonio Otero,[,†] Juan Fernández-Baeza,[*,†] Luis F. Sánchez-Barba,[*,‡] Andrés Garcés,[‡] Agustín Lara-Sánchez[†] and Ana M. Rodríguez[†]*

[†]Departamento de Química Inorgánica, Orgánica y Bioquímica, Universidad de Castilla-La Mancha, Campus Universitario, 13071-Ciudad Real, Spain. [‡]Departamento de Química Inorgánica y Analítica, Universidad Rey Juan Carlos, Móstoles-28933-Madrid, Spain.

E-mail: antonio.otero@uclm.es; juan.fbaeza@uclm.es; luisfernando.sanchezbarba@urjc.es

RECEIVED DATE (to be automatically inserted after your manuscript is accepted if required according to the journal that you are submitting your paper to)

"This document is the unedited Author's version of a Submitted Work that was subsequently accepted for publication in Organometallics, copyright © American Chemical Society after peer review. To access the final edited and published work see http://pubs.acs.org/articlesonrequest/AOR-gN5XJxQtABxZZzvDDdYD."

ABSTRACT

The reaction of enantiopure NNO-scorpionate ligand (*R*,*R*)-bpzmmH with [ZnR_2] (R = Me, Et and CH_2SiMe_3) in a 1:2 molar ratio afforded the dinuclear trisalkyls [Zn(R)(κ^2-NNμ-O)Zn(R)$_2$] (**1**–**3**) [R = Me **1**, Et **2**, CH_2SiMe_3 **3**]. The reaction of the bimetallic trisalkyls **1**–**3** with an aromatic alcohol and thioalcohol yielded the dinuclear zinc complexes containing aryloxide/arylthioxide ligands [(ZnR)$_2$(κN:κN-μ-O)(μ-EAr)] (**4**–**9**) [Ar = 2,6-$C_6H_3Me_2$; E = O, R = Me **4**, Et **5**, CH_2SiMe_3 **6**; E = S, R = Me **7**, Et **8**, CH_2SiMe_3 **9**] by an alcoholysis or thioalcoholysis reaction. The structures of the different compounds were determined by spectroscopic methods and, in addition, the X-ray crystal structures of **2** and **5** were also unambiguously established.

Alkyl and aryloxide/thioaryloxide-containing enantiopure zinc complexes **3**, **4**–**6** and **9** can act as single-component living initiators for the ring-opening polymerization of lactides, affording materials with low molecular weights under mild conditions in only a few hours. Interestingly, microstructural analysis of poly(*rac*-lactide) by ^{1}H NMR spectroscopy revealed that the most sterically hindered initiator [($ZnCH_2SiMe_3$)$_2$(*R*,*R*-bpzmm)(μ-OAr)] (**6**), is one of the first examples of a zinc complex capable of exerting a significant influence on the degree of enantioselectivity, with enriched-isotactic PLAs (P_i = 0.74) produced through an enantiomorphic site control mechanism.

INTRODUCTION

The synthesis of poly(lactide)s (PLAs) is currently being extensively investigated because PLA is one of the most commercially important biodegradable and biocompatible polymers due to its wide array of applications in packaging,[1] microelectronics,[2] and biomedical[3] fields. The increasing interest in this area is evidenced by the number of reviews[4] and books[5] that have been recently published in this field. PLA is an attractive polymer as it can be readily produced from the ring-opening polymerization (ROP) of the bioderived monomer lactide,[6] an inexpensive annually renewable natural feedstock,[6a] and can be degraded to metabolites.[6b,4j]

Given the presence of backbone stereocenters in the lactide diastereoisomers, (*S*,*S*)-LA, (*R*,*R*)-LA and *meso*-LA, as well as the racemic mixture *rac*-lactide, the tacticity of the resulting polymers is one of the main factors that determines the physical and mechanical properties of these polymeric materials, such as thermal resistance, melting temperature and mechanical strength, as well as its rate of chemical and biological degradation.[7] Two possible mechanisms can operate for the stereoselective ROP of lactides and these are chain-end control[8] and enantiomorphic site control[9] mechamisms. Thus, many polymer microstructures such as isotactic,[10,11] atactic,[12,13] syndiotactic[14] and heterotactic[15,16,17] can be constructed from the basic set of diastereoisomers mentioned above. The properties of polylactide are so highly dependent on the polymer tacticity[4] that research into the synthesis of highly selective initiators that are capable of exerting enantiomorphic site control for the ROP of lactides are currently of great interest. In particular, the enantiomorphic polymerization of *rac*-lactide to produce isotactic polylactide is generally limited to trivalent metals supported by chiral ligands, where the Shiff-base (SALEN type)[18] aluminum complexes are clearly dominant,[19] with other metals such as In[20], Y[21] and Nd[22] used to a lesser extent.

Furthermore, given the fact that PLAs are widely utilized in food packaging[1] and biomedical[3] applications, it is preferable to use biocompatible metals such as zinc.[23] In this sense, whereas several highly effective organo-zinc initiators[24] have been described for the efficient ROP of lactides, very few examples of zinc catalysts bearing chiral auxiliaries have been reported,[25-29] and only two have recently succeeded in promoting enantiomorphic site control in the polymerization of *rac*-lactide to poly(isolactide).[28,29] Indeed, our research group has recently explored the reactivity of chiral[30] alkoxo-based[31] scorpionate ligands for the synthesis of well-defined zinc alkyls of the type [Zn(R)(NNO)],[32] which acted as effective single-component living initiators for the ROP of *rac*-lactide, but only a moderately enriched-heterotactic PLA was obtained (P_s = 0.77) by a chain-end control mechanism. However, very recently we, and slightly later Ma *et al*., have communicated the preparation of unprecedented enantiopure hybrid scorpionate/cyclopentadienyl zinc[28] alkyl and an aminophenolate zinc[29] silylamido initiators, respectively, capable to exert a significant preference for isotactic dyad enchainment from *rac*-LA (P_i = 0.77,[28] 0.84[29]). On the basis of these promising

results, we addressed this time the challenge of designing more stereoselective zinc-based catalyst systems[32] supported in this case by this enantiopure NNO-donor scorpionate ligand,[31] which would be capable of exerting higher degrees of enantioselectivity for the production of isotactic polylactide from *rac*-lactide through an enantiomorphic site control mechanism.

Herein we describe the preparation and structural characterization of new enatiopure NNO-scorpionate alkyl and alkyl-aryloxide/arylthioxide zinc complexes of the type [Zn(R)(κ^2-NNμ-O)Zn($R)_2$] and [($ZnR)_2$(κN:κN-μ-O)(μ-EAr)] (E = O, S), respectively, as single-component living initiators for the stereocontrolled ROP of *rac*-lactide in the production of isotactic polylactide.

RESULTS AND DISCUSSION

Reaction of the alcohol enantiopure-scorpionate compound (*R*,*R*)-bpzmmH[31] {(*R*,*R*)-bpzmmH = (1*R*)-1-[(1*R*)-6,6-dimethylbicyclo[3.1.1]-2-hepten-2-yl]-2,2-bis(3,5-dimethylpyrazol-1-yl)ethanol} with [ZnR_2] (R = Me, Et, CH_2SiMe_3) in a 1:2 molar ratio in toluene or diethyl ether afforded, after the appropriate work-up, the dinuclear enantiopure alkyl zinc complexes [Zn(R)(κ^2-NNμ-O)Zn($R)_2$] (**1**–**3**) (see Scheme 1).

Some aspects concerning the reactivity of the isolated zinc metal complexes were also considered. For instance, we explored the reactivity of [Zn(R)(κ^2-NNμ-O)Zn($R)_2$] (**1**–**3**) with several aromatic alcohols or thioalcohols and we prepared aryloxide or arylthioxide derivatives of scorpionate-containing compounds in an alcoholysis or thioalcoholysis reaction with ArEH (1 equiv; E = O, S; Ar = 2,6-$C_6H_3Me_2$) to yield the dinuclear enantiopure zinc complexes [($ZnR)_2$(κN:κN-μ-O)(μ-EAr)] (**4**–**9**) (see Scheme 1). However, the reaction of **1**–**3** with aliphatic alcohols, such as methanol or isopropanol, in different molar ratios and under different conditions, proved unsuccessful.

Scheme 1. Synthesis of enantiopure NNO-scorpionate alkyl zinc complexes (**1–9**).

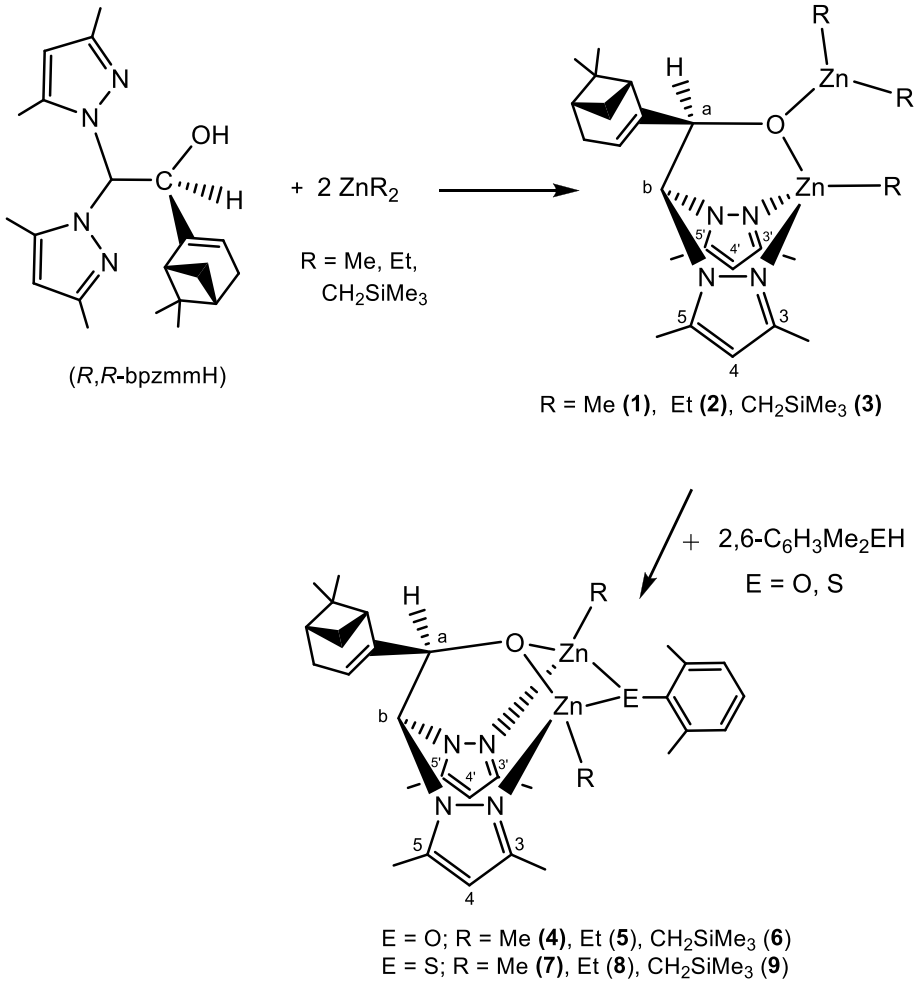

The different complexes were characterized spectroscopically. The ^{1}H and $^{13}C\{^{1}H\}$ NMR spectra of **1**–**9** exhibit two distinct sets of pyrazole resonances, indicating the existence of two types

of pyrazole rings. The ^{1}H NMR spectra of these complexes show two singlets for each of the H^{4}, Me^{3} and Me^{5} pyrazole protons, one broad singlet for each of the methine groups (the CH^{b} bridge of the two pyrazole rings and the chiral carbon CH^{a}) and the signals corresponding to the bicycle moiety of the scorpionate ligand and the alkyl or aryloxide ligands. These results are consistent with a geometric environment for the zinc atoms in which the two pyrazole rings are located in *cis* and *trans* positions with respect to the bicyclic group (see Scheme 1). The ^{1}H NOESY-1D experiments enabled the unequivocal assignment of all ^{1}H resonances, and the assignment of the $^{13}C\{H\}$ NMR signals was carried out on the basis of ^{1}H-^{13}C heteronuclear correlation (g-HSQC) experiments. In addition, the presence in solution of only one enantiomer for these complexes was confirmed by the addition of a chiral shift reagent, since this addition did not modify the ^{1}H NMR spectra of these compounds.

Complexes **2** and **5** were also characterized by single-crystal X-ray diffraction and the molecular structures are shown in Figures 1 and 2, respectively. These studies confirmed that the enantiopure character of these complexes in solution is maintained in the solid-state. The most representative bond lengths and angles are presented in Table 1. (Crystallographic details are included in Table S3 in the Supporting Information). The complex **2** has a dinuclear structure in the solid state with a μ-bridging alkoxide in between the two four- and three-coordinate Zn(II) centers. The first zinc center Zn(1) has a distorted tetrahedral geometry with a heteroscorpionate ligand that acts in a tridentate fashion. The pyrazolic nitrogens N(1) and N(3) occupy two positions and the alkoxide oxygen-bridge μ-O(1) and the ethyl group the other two positions. The second zinc center has a distorted trigonal geometry, in which μ-O(1) occupies one position and the alkyl groups the other two positions. As far as we know, only one structure with two four- and three-coordinate Zn(II) atoms, bonded by only one bridging oxygen atom, has previously been reported in the literature.[33] Finally, the scorpionate ligand retains the *R*-configuration at the C^{a} (C12) atom in complex **2**, thus confirming its enantiopure character.

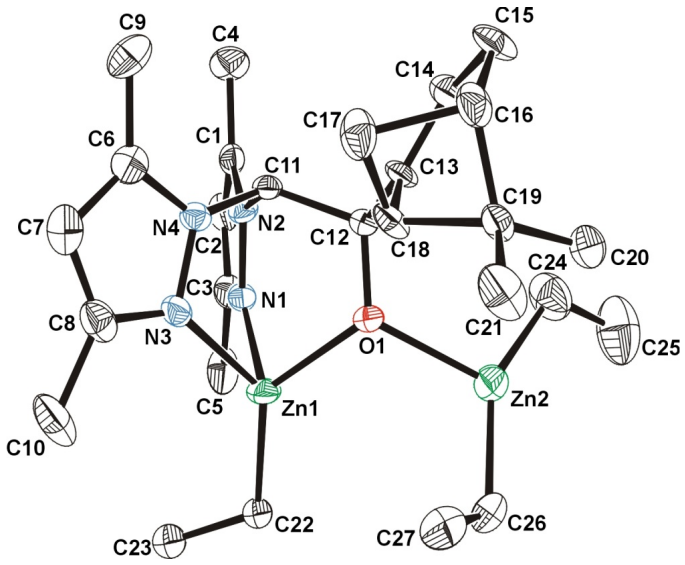

Figure 1. ORTEP view of enantiopure complex [Zn(Et)(*R*,*R*-bpzmm)Zn(Et)$_2$] (**2**). Hydrogen atoms have been omitted for clarity. Thermal ellipsoids are drawn at the 30% probability level.

Table 1. Selected bond lengths (Å) and angles (º) for **2** and **5**.

2		**5**	
Bond lengths			
Zn(1)–O(1)	1.974(4)	Zn(1)-O(1)	2.016(2)
Zn(1)–N(1)	2.104(7)	Zn(1)-O(2)	2.018(2)
Zn(1)–N(3)	2.106(7)	Zn(1)-N(3)	2.108(3)
Zn(1)–C(22)	2.01(1)	Zn(1)-C(30)	1.977(4)
Zn(2)–O(1)	2.099(4)	Zn(2)-N(1)	2.144(3)
Zn(2)–C(24)	1.99(1)	Zn(2)-C(32)	1.979(4)
Zn(2)–C(26)	2.000(9)	O(1)-C(12)	1.391(4)
O(1)–C(12)	1.394(6)	Zn(2)-O(1)	2.005(2)
		Zn(2)-O(2)	2.007(2)
Angles			
O(1)–Zn(1)–N(1)	89.7(2)	O(1)-Zn(1)-O(2)	83.46(9)
O(1)–Zn(1)–N(3)	88.9(2)	C(30)-Zn(1)-O(1)	135.8(1)
O(1)–Zn(1)–C(22)	131.0(5)	C(30)-Zn(1)-O(2)	123.0(1)

C(22)–Zn(1)–N(1)	109.4(5)	C(30)-Zn(1)-N(3)	117.9(1)
C(22)–Zn(1)–N(3)	134.9(5)	O(1)-Zn(1)-N(3)	88.6(1)
C(24)–Zn(2)–O(1)	105.4(3)	O(2)-Zn(1)-N(3)	97.4(1)
C(26)–Zn(2)–O(1)	106.4(3)	C(32)-Zn(2)-O(1)	134.1(1)
C(24)–Zn(2)–C(26)	148.0(4)	C(32)-Zn(2)-O(2)	119.1(1)
Zn(1)–O(1)–Zn(2)	112.9(2)	O(1)-Zn(2)-O(2)	84.02(9)
C(12)–O(1)–Zn(1)	119.8(4)	C(32)-Zn(2)-N(1)	117.9(1)
C(12)–O(1)–Zn(2)	119.4(4)	O(1)-Zn(2)-N(1)	89.6(1)
		O(2)-Zn(2)-N(1)	104.3(1)
		Zn(2)-O(1)-Zn(1)	96.1(1)
		C(12)-O(1)-Zn(2)	122.9(2)
		C(12)-O(1)-Zn(1)	119.7(2)
		C(22)-O(2)-Zn(2)	132.6(2)
		C(22)-O(2)-Zn(1)	126.5(2)
		Zn(2)-O(2)-Zn(1)	96.0(1)

The X-ray structure analyses of complex **5** revealed that this molecule has a rhomboidal $(ZnO)_2$ core with clearly different Zn(1)–O(1) or O(2) and Zn(2)–O(1) or O(2) Å bond lengths, ranging from 2.005(2) to 2.018(2) Å, respectively, with the Zn···Zn diagonal (2.992 Å) much longer than the O···O diagonal (2.685 Å). The coordination environment of each Zn atom can be described as a distorted tetrahedron with a heteroscorpionate ligand that acts in a tridentate fashion (two coordinated pyrazole rings bridge the two zinc atoms and the oxygen atom from the alkoxide fragment, which also bridges the two zinc atoms), and the other two coordination positions of the two zinc atoms are completed with an oxygen atom from the aryloxide ligand, bridging the two zinc atoms, and finally, an ethyl ligand on each zinc atom. The dimeric aggregate is based on Zn_2O_2 four-membered rings, which have previously been observed in other zinc compounds that contain, for

example, thiolate-oxo,[34] alkoxide-imino,[35] aryloxide[36] or aminoalcoholate[37] ligands and, more recently, in our research group with dinuclear complexes of the type [Zn(R)(κ-NNμ-O)]$_2$.[32]

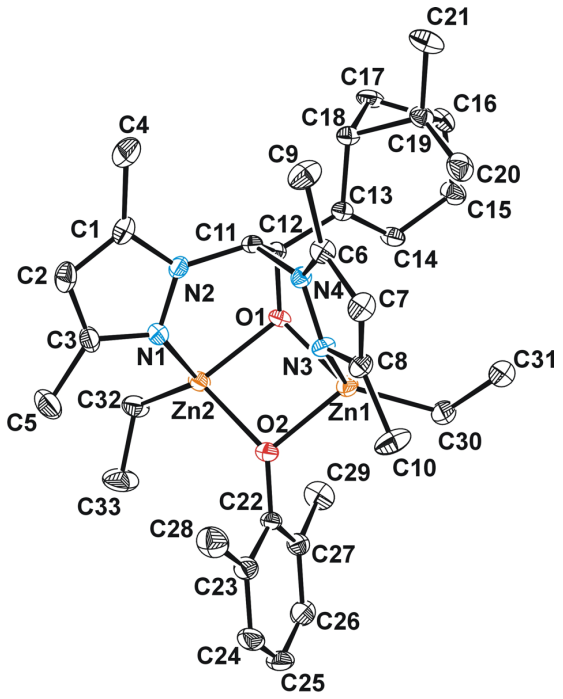

Figure 2. ORTEP view of enantiopure complex [(ZnEt)$_2$(*R*,*R*-bpzmm)(μ-OAr)] (**5**). Hydrogen atoms have been omitted for clarity. Thermal ellipsoids are drawn at the 30% probability level.

Polymerization Studies. Complexes **3**, **4**–**6** and **9** were systematically assessed in the ring-opening polymerization of the polar monomers L-/*rac*-lactide (LA) for the production of poly(lactides) (PLAs). Inspection of the experimental M_n values of the PLAs produced reveals, as a common trend, that the molecular weights of the resulting polymer samples closely approximate the expected theoretical calculated values for one growing polymer chain per catalyst molecule [M_n(calcd)PLA$_{100}$ = 14 400 g·mol^{-1}]. Size exclusion chromatography (SEC) data for the resulting polyesters show a monomodal weight distribution, with polydispersities ranging from 1.02 to 1.16.

Thus, **3** and **4**–**6** acted as active single-component living catalysts for the well-controlled polymerization of L-LA in tetrahydrofuran under mild conditions (50ºC) (see Table S1 in the SI). For instance, the zinc alkyl derivative **3** polymerized 67% of the monomer after 1h, yielding low molecular weight polymer with narrow molecular weight distribution. The NNO-donor alkyl-

aryloxide catalysts **4**–**6** gave comparable productivity values under similar conditions. These reactions afforded highly crystalline, isotactic polymers (T_m = 169–177 ºC)[38] with low-medium molecular weight. The high level of control afforded by these initiators in the polymerization of L-lactide was further exemplified by the narrow molecular weight distributions (see Figure S1 in the SI) in conjunction with linear correlations between M_n and percentage conversion (R^2 = 0.989) for catalyst **5** (see Figure S2 in the SI). A double-feed experiment demonstrated the living behavior of this initiator (see Table S1 in the SI), which resulted in a polymer chain extension[39] with very similar polymer features. Additionally, low molecular weight materials produced by initiator **5** were studied by Matrix-Assisted Laser Desorption/Ionization Time-of-Flight Mass Spectrometry (MALDI-ToF MS)[40] (see Figure S3 in the SI) as well as end-group analysis by ^{1}H NMR of a poly(L-lactide) oligomer was also investigated (see Figure S4 in the SI). These two findings provide evidence that the ring-opening of L-LA occurs by the initial addition of the aryloxide fragment, rather than the alkyl ligand, to the monomer in the materials produced, with cleavage of the acyl-oxygen bond[41] followed by further monomer additions to the (macro)alcohols. Kinetic studies conducted for the ROP of L-LA employing **5** and **6** at 50ºC established that the reaction order with respect to monomer and catalyst concentration follows a first-order dependence (square correlation coefficients ≥ 0.97) (see Figures S5a, S6a and Table S2 in the SI). Interestingly, the pseudo-first-order rate constants, k_{app}, for each initiator are significantly higher than that measured for the analogous chiral monoalkyls $[Zn(R)(NNO)]_2$[32] ($k_{app,50ºC}$= 8.3 ± 0.3 × 10^{-4} s^{-1}, R = CH_2SiMe_3 *vs* $k_{app,50ºC}$= 38 ± 2 × 10^{-4} s^{-1} for **6**, at a $[Zn]_0$ = 20 mM). It is also noteworthy the similarity between the experimentally obtained k_{app} values for initiators **5** and **6** in the polymerization of L-LA at each $[catalyst]_0$ studied (see Table S2 in the SI), which provides additional evidence that the initiation step in the ROP of lactide is mediated by the aryloxide/thioaryloxide group rather than an alkyl group in complexes **4**–**9**.

Finally, initiators **3**, **4**–**6** and **9** were also tested in the polymerization of *rac*-lactide in tetrahydrofuran at 20ºC and 50ºC (Table 2). For instance, the alkyl catalyst **3** proved to be active at 50ºC, reaching a 50% of conversion after 4 hours of reaction, with production of low molecular weight materials with narrow polydispersity values (M_n = 7 500, M_w/M_n = 1.09, entry 1). In contrast,

the catalytic activity of the heteroscorpionate mixed ligand alkyl-aryloxide zinc derivatives **4**–**6** did not vary uniformly and was found to depend on the electronic and steric effects exerted by both alkyls on the aryloxide leaving group. Thus, whereas catalyst **4** was active at 20ºC, **5** and **6** required 50ºC to transformed ~25% of the monomer after 1 and 2 hours, respectively, with very narrow molecular weight distributions. As a general trend, after the 4 hour of reaction time investigated, neither of the catalysts exceeded 50% conversion. Additionally, the thioaryloxide derivative **9** clearly presented a lower catalytic activity, possibly due to partial catalyst decomposition at the reaction temperature. In this monomer, the kinetic determinations for **5** and **6** at the same temperature than for L-LA also confirmed first-order dependence with respect to monomer and catalyst concentration ($r^2 \geq 0.97$) (see Figure S5b , S6b and Table S2 in the SI). In addition, the agreement between the k_{app} values observed for L- and *rac*-LA polymerizations for each initiator studied indicates that preferentially L-LA is converted when *rac*-LA is polymerized. These data parallels the fact that extension of the reaction time up to 24 hours for initiator **6** only led to an increase in conversion up to 59% (Table 2, entry 7), thus showing that the D-lactide monomer is polymerized very slowly. Nonetheless, the k_{app} values observed for **6** are slightly lower than that determined for **5** in *rac*-lactide monomer, probably as a result of the higher steric hindrance of the alkyl groups on **6**, which permanently delay the coordination of the incoming lactide monomer to both zinc centers. In general terms, the melting points and the rotation angles measured for the poly(*rac*-lactide)s increase with the isotactic level of the materials [see below for the Poly(*rac*-lactide) Microstructure Analysis], reaching a value of T_m = 166ºC and $[\alpha]_D^{22}$ = –103 in the case of **6**, which clearly indicates a significant degree of isotacticity in the polymer microstructure.

For the sake of comparison, the mixed ligand alkyl-aryloxide zinc derivatives **4**–**6** present comparable activity with the enantiopure hybrid scorpionate/cyclopentadienyl zinc alkyl [ZnEt(κ^2-$\eta^1(\pi)$-*R,S*-bpmycp)],[28] but higher than the analogous zinc monoalkyls,[13,15,32] all of them recently reported by our group. They are also more active than alternative robust zinc guanidine complexes of the type [Zn(guanidine)$_2$OTf]OTf[42] or recently published zinc alkyls supported by *N*,*O*-bidentate ligands [(κ^2-N,O)ZnEt],[24c] which need more energetic conditions and longer reaction times to

produce lower conversions of material. However, the activity of these initiators is still far from that for the most heralded organo-zinc initiators[17b,24i,j,29] reported in the literature.

Table 2. Polymerization of *rac*-Lactide Catalyzed by 3, 4–6 and 9.[a]

entry	initiator	temp (°C)	time (h)	yield (g)	conv (%)[b]	$M_{n(theor)}$ (Da)[c]	M_n (Da)[d]	M_w/M_n[d]	P_i[e]
1	**3**	50	4	0.65	50	7 200	7 500	1.09	0.52
2	**4**	20	4	0.49	38	5 500	5 200	1.07	0.59
3	**5**	20	4	traces	-	-	-	-	-
4	**5**	50	1	0.30	23	3 300	3 700	1.02	0.61
5	**6**	50	2	0.32	25	3 600	3 400	1.03	0.74
6	**6**	50	4	0.62	48	6 900	6 800	1.05	0.73
7	**9**	50	4	0.32	25	3 600	3 800	1.15	0.71

[a] Polymerization conditions: in all cases the $[catalyst]_0$ refers to the initiating species, which includes both Zn centers per initiator: 90 μmol of catalyst, 10 mL of tetrahydrofuran as solvent, $[rac\text{-lactide}]_0/[catalyst]_0 = 100$. [b] Percentage conversion of the monomer [(weight of polymer recovered/weight of monomer) × 100]. [c] Theoretical M_n = (monomer/catalyst) × (% conversion) × (M_w of lactide). [d] Determined by size exclusion chromatography relative to polystyrene standards in tetrahydrofuran. Experimental M_n was calculated considering Mark–Houwink's corrections[43] for M_n [$M_n(obsd) = 0.56 \times M_n(GPC)$]. [e] The parameter P_i (i = isotactic) is the probability of forming a new *i*-dyad. The P_i and the P_s (s = syndiotactic) values were calculated from the following tetrads probabilities based on enantiomophic site control statistics[44] in the polymerization of *rac*-lactide: *sis, sii, iis* = $[P_i^2(1\text{-}P_i)+P_i(1\text{-}P_i)^2]/2$; *iii* = $[P_i^2(1\text{-}P_i)^2+P_i^3+(1\text{-}P_i)^3]/2$; *isi* = $[P_i(1\text{-}P_i)+P_i(1\text{-}P_i)]/2$.

Poly(*rac*-lactide) Microstructure Analysis. Microstructural analysis by homonuclear decoupled ^{1}H NMR spectroscopy on the poly(*rac*-lactide)s[14a,b,45] revealed that while the enantiomerically pure trisalkyl **3** did not exert sterocontrol and essentially atactic material was obtained (P_i = 0.52, Table 2, entry 1), the corresponding derivatives alkyl-aryloxides **5** and **6** and the alkyl-thioaryloxide **9** impart a preference for an isotactic dyad enchainment. The P_i values were calculated according to the Coudane *et al*.[46] method. Thus, initiator **6** afforded a P_i value of 0.74 (Figure S7 in the SI, Table 2, entry 5), which indicates that the polymer contained an average of 8 units (Ł ≈ 8) of enantiomerically pure L-lactide {Ł = 2/(1 – P_i)},[46] and in the case of **9**, the value was 0.71 (Table 2, entry 7, Ł ≈ 7). Additionally, analysis of the methine region allowed the mechanism of stereocontrol to be determined: *i.e*., enantiomorphic site control[9] *vs* chain end control.[8] This was assessed by analysis of the tetrads resulting from stereoerrors (*i.e*., tetrads other than *iii*). Analysis of the isotactic PLA produced by the most selective initiator **6** indicates that an enantiomorphic site control mechanism[9,19a] is dominant ([*sis*]/[*sii*]/[*iis*]/[*isi*] = 1/1/1/2 ratio (Figure S7 in the SI). This interesting step forward obtained for catalysts **6** and **9**, under these conditions, is most probably the result of the high homosteric control caused by both the myrtenal fragment in the NNO-donor heteroscorpionate ligand and the two sterically demanding trimethylsilylmethyl alkyls around the two catalytic zinc metal centers.

CONCLUSIONS

The reaction of an enantiopure bis(pyrazol-1-yl)methane-based NNO-donor scorpionate alcohol with [ZnR_2] has led to the preparation of new dinuclear zinc trisalkyls [Zn(R)(κ^2-NNμ-O)Zn($R)_2$]. Subsequent reaction with a phenol/thiophenol yielded a family of mixed ligand alkyl-aryloxide/thioaryloxide complexes [($ZnR)_2$(κN:κN-μ-O)(μ-EAr)] (E = O, S). These families of enantiomerically pure alkyl or alkyl-aryloxide/thioaryloxide zinc complexes can act as single-site living initiators for the well-controlled polymerization of lactides under mild conditions in a few hours. Interestingly, microstructural analysis of the materials revealed that these initiators promote

enhanced degrees of isoactivity. In particular, the most sterically hindered initiators **6** and **9** produce isotactic-enriched PLAs (P_i = 0.74 and 0.71, respectively). These results constitute one of the first examples of enantiomerically pure zinc initiators capable of exerting significant levels of stereocontrol in the growing polymer microstructures through an enantiomorphic site control mechanism.

EXPERIMENTAL SECTION

All manipulations were carried out under a nitrogen atmosphere using standard Schlenk techniques or a glovebox. Solvents were predried over sodium wire and distilled under nitrogen from sodium (toluene and *n*-hexane) or sodium-benzophenone (THF and diethyl ether). Deuterated solvents were stored over activated 4 Å molecular sieves and degassed by several freeze-thaw cycles. NMR spectra were recorded on a Varian Inova FT-500 spectrometer and are referenced to the residual deuterated solvent. ^{1}H NMR homodecoupled and NOESY-1D spectra were recorded on the same instrument with the following acquisition parameters: irradiation time 2 s and 256 scans, using standard VARIAN-FT software. 2D NMR spectra were acquired using the same software and processed using an IPC-Sun computer. Microanalyses were performed with a Perkin-Elmer 2400 CHN analyzer. Gel Permeation Chromatography (GPC) measurements were performed on a Shimadzu LC-20AD instrument equipped with a TSK-GEL G3000H column and an ELSD-LTII light-scattering detector. The GPC column was eluted with THF at 40ºC at 1 mL/min and was calibrated using eight monodisperse polystyrene standards in the range 580–483 000 Da. MALDI-ToF MS data were acquired with a Bruker Autoflex II ToF/ToF spectrometer, using a nitrogen laser source (337 nm, 3 ns) in linear mode with a positive acceleration voltage of 20 kV. Samples were prepared as follows: PLA (20 mg) was dissolved in HPLC quality THF with matrix and NaI in a 100:5:5 ratio. Before evaporation, 10 μL of the mixture solution was deposited on the sample plate. External calibration was performed by using Peptide Calibration Standard II (covered mass range: 700–3 200 Da) and Protein Calibration Standard I (covered mass range: 5 000–17 500 Da). The microstructures of PLA samples were determined by examination of the methine region in the homodecoupled ^{1}H NMR

spectrum of the polymers recorded at room temperature in $CDCl_3$ on a Varian Inova FT-500 spectrometer. The starting material (*R*,*R*)-bpzmmH[31] was also prepared according to literature procedures. Reagents $ZnCl_2$ anhydrous, $ZnMe_2$, $ZnEt_2$ (Aldrich) and $LiCH_2SiMe_3$ (Acros) were used as purchased. $Zn(CH_2SiMe_3)_2$ was prepared according to literature procedures.[15,47] 2,6-Dimethylphenol was sublimed twice under reduced pressure and stored in a glovebox. 2,6-Dimethylthiophenol was degassed by several freeze thaw cycles and stored over 4 Å molecular sieves. L-Lactide and *rac*-lactide were sublimed twice, recrystallized from THF and finally sublimed again prior to use.

Preparation of compounds 1–9.

Synthesis of [Zn(Me)(*R*,*R*-bpzmm)Zn(Me)$_2$] (1). In a 250 cm^3 Schlenk tube, *R*,*R*-bpzmmH (1.0 g, 2.82 mmol), was dissolved in dry toluene (60 mL) and the solution was cooled to –70 ºC. A solution of $ZnMe_2$ (2.0 M in toluene, 2.82 mL, 5.64 mmol) was added and the mixture was allowed to warm up to room temperature and stirred during 2 h. The solvent was evaporated to dryness under reduced pressure to yield a sticky white product. The product was washed with *n*-hexane (1 × 20 mL) to give compound **1** as white solid. Yield: 1.33 g (89%). ^{1}H NMR (C_6D_6, 297 K), δ 5.77 (bs, 1H, CH^b), 5.63 (bs, 1H, CH^a), 5.35 (s, 1H, H$^{4'}$), 5.32 (s, 1H, H^4), 5.17 (bs, 1H, H^d), 2.22 (m, 4H, H^{e,f,i}), 2.02 (s, 3H, Me$^{3'}$), 1.98 (s, 3H, Me^3), 1.96 (bs, 1H, H^h), 1.68 (s, 3H, Me$^{5'}$), 1.64 (s, 3H, Me^5), 1.24 (s, 3H, Me^j), 0.95 (s, 3H, Me^k), 0.82 (d, 1H, $^2J_{H\text{-}H}$ = 8.4Hz, H^h), 0.11 (bs, 3H, Zn-$\underline{CH_3}$), –0.17 (bs, 6H, Zn-($\underline{CH_3}$)$_2$). ^{13}C {^{1}H} NMR (C_6D_6, 297 K), δ 151.3–138.5 (C$^{3,3'}$, C$^{5,5'}$), 149.3 (C^d), 139.8 (C^c), 105.9 (C$^{4'}$), 105.7 (C^4), 80.5 (C^a), 68.8 (C^b), 41.5 (C^f), 41.2 (C^i), 38.2 (C^g, C^e), 32.2 (C^h), 26.3 (Me^k), 21.6 (Me^j), 12.6 (Me^3), 12.5 (Me$^{3'}$), 10.5 (Me$^{5'}$), 10.1 (Me^5), –2.4 (Zn-$\underline{CH_3}$), –15.3 (Zn-($\underline{CH_3}$)$_2$). Elemental analysis (%) calcd for $C_{24}H_{38}N_4OZn_2$: C, 54.46; H, 7.24; N, 10.58. Found: C, 54.46; H, 7.25; N, 10.56. $[\alpha]_D^{22}$ = +30.8 (*c* 10^{-3} g/mL, toluene).

Synthesis of [Zn(Et)(*R*,*R*-bpzmm)Zn(Et)$_2$] (2). The synthesis of **2** was carried out in an identical manner to **1**, but **2** was obtained as colorless crystals from toluene at –26 ºC. *R*,*R*-bpzmmH (1.0 g, 2.82 mmol), $ZnEt_2$ (1.0 M in *n*-hexane, 5.64 mL, 5.64 mmol). Yield: 1.46 g (91%). ^{1}H NMR (C_6D_6,

297 K), δ 5.75 (bs, 1H, CH^{b}), 5.58 (bs, 1H, CH^{a}), 5.38 (s, 1H, H$^{4'}$), 5.33 (s, 1H, H^{4}), 5.09 (bs, 1H, H^{d}), 2.20 (m, 4H, H^{e,f,i}), 2.06 (s, 3H, Me$^{3'}$), 2.04 (s, 3H, Me^{3}), 1.96 (bs, 1H, H^{h}), 1.87, (t, 3H, $^{3}J_{H\text{-}H}$ = 8.1 Hz, Zn-CH$_2$CH$_3$), 1.71 (t, 6H, $^{3}J_{H\text{-}H}$ = 8.1 Hz, Zn-(CH$_2$CH$_3$)$_2$), 1.69 (s, 3H, Me$^{5'}$), 1.66 (s, 3H, Me^{5}), 1.27 (s, 3H, Me^{j}), 0.98 (s, 3H, Me^{k}), 0.97 (q, 4H, $^{3}J_{H\text{-}H}$ = 8.1 Hz, Zn-(CH$_2$CH$_3$)$_2$), 0.82 (d, 1H, $^{2}J_{H\text{-}H}$ = 8.1 Hz, H^{h}), 0.68 (q, 1H, $^{3}J_{H\text{-}H}$ = 8.1 Hz, Zn-CH$_2$CH$_3$), 0.58 (q, 1H, $^{3}J_{H\text{-}H}$ = 8.1 Hz, Zn-CH$_2$CH$_3$). ^{13}C {^{1}H} NMR (C_6D_6, 297 K), δ 152.3–138.4 (C$^{3,3'}$, C$^{5,5'}$), 149.0 (C^{d}), 139.6 (C^{c}), 105.8 (C$^{4'}$), 105.6 (C^{4}), 80.9 (C^{a}), 69.1 (C^{b}), 41.6 (C^{f}), 41.1 (C^{i}), 38.2 (C^{g}, C^{e}), 32.3 (C^{h}), 31.6 (Me^{k}), 21.3 (Me^{j}), 13.6 (Zn-CH$_2$CH$_3$), 13.2 (Zn-(CH$_2$CH$_3$)$_2$), 12.7 (Me^{3}), 12.3 (Me$^{3'}$), 10.5 (Me$^{5'}$), 10.1 (Me^{5}), 3.8 (Zn-CH$_2$CH$_3$), –2.0 (Zn-(CH$_2$CH$_3$)$_2$). Elemental analysis (%) calcd for $C_{27}H_{44}N_4OZn_2$: C, 56.75; H, 7.76; N, 9.80. Found: C, 56.80; H, 7.78; N, 9.78. $[\alpha]_D^{22}$ = +29.9 (*c* 10^{-3} g/mL, toluene).

Synthesis of [Zn(CH$_2$SiMe$_3$)(*R*,*R*-bpzmm)Zn(CH$_2$SiMe$_3$)$_2$] (3). The synthesis of **3** was carried out in an identical manner to **1**, but **3** was obtained as pale yellow solid. bpzmmH (1.0 g, 2.82 mmol), [Zn(CH$_2$SiMe$_3$)$_2$] (1.8 M in Et$_2$O, 3.13 mL, 5.64 mmol). Yield: 1.89 g (90%). ^{1}H NMR (C_6D_6, 297 K), δ 5.73 (bs, 1H, CH^{b}), 5.68 (bs, 1H, CH^{a}), 5.41 (s, 1H, H$^{4'}$), 5.29 (s, 1H, H^{4}), 5.08 (bs, 1H, H^{d}), 2.20 (m, 4H, H^{e,f,i}), 2.10 (s, 3H, Me$^{3'}$), 2.08 (s, 3H, Me^{3}), 1.93 (bs, 2H, H^{h}), 1.74 (s, 3H, Me$^{5'}$), 1.60 (s, 3H, Me^{3}), 1.32 (s, 3H, Me^{j}), 0.88 (s, 3H, Me^{k}), 0.78 (d, 1H, $^{2}J_{H\text{-}H}$ = 8.4 Hz, H^{h}), 0.46 (s, 9H, Zn-CH$_2$SiMe$_3$), 0.30 (s, 18H, Zn-(CH$_2$SiMe$_3$)$_2$), –0.20 (d, 1H, $^{2}J_{H\text{-}H}$ = 12.3 Hz, Zn-CH$_2$SiMe$_3$), –0.31 (d, 1H, $^{2}J_{H\text{-}H}$ = 12.3 Hz, Zn-CH$_2$SiMe$_3$), –0.54 (d, 2H, $^{2}J_{H\text{-}H}$ = 12.3 Hz, Zn-(CH$_2$SiMe$_3$)$_2$), –0.62 (d, 2H, $^{2}J_{H\text{-}H}$ = 12.3 Hz, Zn-(CH$_2$SiMe$_3$)$_2$). ^{13}C {^{1}H} NMR (C_6D_6, 297 K), δ 151.8–137.4 (C$^{3,3'}$, C$^{5,5'}$), 148.7 (C^{d}), 139.5 (C^{c}), 105.8 (C$^{4'}$), 105.6 (C^{4}), 80.4 (C^{a}), 70.0 (C^{b}), 41.8 (C^{f}), 41.1 (C^{i}), 38.9 (C^{g}, C^{e}), 32.1 (C^{h}), 31.6 (Me^{k}), 21.9 (Me^{j}), 12.9 (Me^{3}), 12.3 (Me$^{3'}$), 10.4 (Me$^{5'}$), 10.1 (Me^{5}), 4.5 (Zn-CH$_2$SiMe$_3$), 3.8 (Zn-(CH$_2$SiMe$_3$)$_2$), –0.5 (Zn-CH$_2$SiMe$_3$), –9.0 (Zn-(CH$_2$SiMe$_3$)$_2$). Elemental analysis (%) calcd for $C_{33}H_{62}N_4OSi_3Zn_2$: C, 53.13; H, 8.38; N, 7.51. Found: C, 53.16; H, 8.42; N, 7.55. $[\alpha]_D^{22}$ = +30.3 (*c* 10^{-3} g/mL, toluene).

Synthesis of [(ZnMe)$_2$(*R*,*R*-bpzmm)(OAr)] (4). In a 250 cm^3 Schlenk tube, [Zn(Me)(bpzmm)Zn(Me)$_2$] (1.0 g, 1.89 mmol) was dissolved in dry toluene (60 mL) and the

solution was cooled to −70 ºC. In another 100 mL Schlenk tube, 2,6-dimethylphenol (0.23 g, 1.89 mmol) was dissolved in dry toluene (20 mL) and precooled to −20 ºC. The solution of 2,6-dimethylphenol was added dropwise to the [Zn(Me)(bpzmm)Zn(Me)$_2$] solution and the mixture was allowed to warm up to room temperature and stirred during 10 min. The solvent was evaporated to dryness under reduced pressure to yield a pale yellow product, which was washed with *n*-hexane (1 × 15mL) to give compound **4** as white solid. Yield: 1.07 g (89%). ^{1}H NMR (C_6D_6, 297 K), δ 7.21 (d, 2H, $^3J_{H\text{-}H}$ = 7.1 Hz, *m*-H-OAr), 6.86 (t, 1H, $^3J_{H\text{-}H}$ = 7.1 Hz, *p*-H-OAr), 5.62 (bs, 2H, CH^b, CH^a), 5.37 (s, 1H, H$^{4'}$), 5.34 (s, 1H, H^4), 5.15 (bs, 1H, H^d), 2.51 (bs, 6H, $\underline{CH_3}$-OAr), 2.25–2.20 (m, 4H, H^{e,f,i}), 2.06 (s, 3H, Me$^{3'}$), 1.98 (s, 3H, Me^3), 1.94 (d, 1H, $^2J_{H\text{-}H}$ = 8.4 Hz, H^h), 1.65 (s, 3H, Me$^{5'}$), 1.42 (s, 3H, Me^5), 1.25 (s, 3H, Me^j), 1.04 (d, 1H, $^2J_{H\text{-}H}$ = 8.4 Hz, H^h), 0.83 (s, 3H, Me^k), –0.25 (bs, 3H, Zn-$\underline{CH_3}$), –0.35 (bs, 3H, Zn-$\underline{CH_3}$). ^{13}C {^{1}H} NMR (C_6D_6, 297 K), δ 160.6 (C_{ipso}-OAr), 152.3–137.8 (C$^{3,3'}$, C$^{5,5'}$), 149.0 (C^d), 141.2 (C^c), 129.2 (*o*-C-OAr), 125.6 (*m*-C-OAr), 118.0 (*p*-C-OAr), 107.4 (C$^{4'}$), 107.1 (C^4), 79.0 (C^a), 69.14 (C^b), 41.9 (C^f), 41.4 (C^i), 38.2 (C^g, C^e), 32.2 (C^h), 26.3 (Me^k), 21.3 (Me^j), 17.8 ($\underline{CH_3}$-OAr), 13.6 (Me^3), 13.5 (Me$^{3'}$), 11.5 (Me$^{5'}$), 11.0 (Me^5), –13.5 (Zn-$\underline{Me}$), –14.4 (Zn-$\underline{Me}$). Elemental analysis (%) calcd for $C_{31}H_{44}N_4O_2Zn_2$: C, 58.59; H, 6.98; N, 8.82. Found: C, 58.65; H, 7.00; N, 8.89. $[\alpha]_D^{22}$ = +32.0 (*c* 10^{-3} g/mL, toluene).

Synthesis of [(ZnEt)$_2$(*R*,*R*-bpzmm)(OAr)] (5). The synthesis of **5** was carried out in an identical manner to **4**, but **5** was obtained as colorless crystals from a mixture of toluene/*n*-hexane (1:3) at −26 ºC. [Zn(Et)(bpzmm)Zn(Et)$_2$] (1.0 g, 1.75 mmol), 2,6-dimethylphenol (0.21 g, 1.75 mmol). Yield: 1.00 g (86%). ^{1}H NMR (C_6D_6, 297 K), δ 7.19 (d, 2H, $^3J_{H\text{-}H}$ = 7.1 Hz, *m*-H-OAr), 6.83 (t, 1H, $^3J_{H\text{-}H}$ = 7.1 Hz, *p*-H-OAr), 5.76 (bs, 2H, CH^b, CH^a), 5.40 (s, 1H, H$^{4'}$), 5.36 (s, 1H, H^4), 5.12 (bs, 1H, H^d), 2.47 (bs, 6H, $\underline{CH_3}$-OAr), 2.30–2.25 (m, 4H, H^{e,f,i}), 2.08 (s, 3H, Me$^{3'}$), 2.0 (s, 3H, Me^3), 1.94 (bs, 1H, H^h), 1.66 (bs, 3H, Zn-CH$_2\underline{CH_3}$), 1.65 (s, 3H, Me$^{5'}$), 1.42 (s, 3H, Me^5), 1.40 (bs, 3H, Zn-CH$_2\underline{CH_3}$), 1.27 (s, 3H, Me^j), 1.04 (d, 1H, $^2J_{H\text{-}H}$ = 8.4 Hz, H^h), 0.88 (s, 3H, Me^k), 0.75 (bs, 2H, Zn-$\underline{CH_2}$CH$_3$), 0.58 (bs, 2H, Zn-$\underline{CH_2}$CH$_3$). ^{13}C {^{1}H} NMR (C_6D_6, 297 K), δ 162.3 (C_{ipso}-OAr), 151.6–136.8 (C$^{3,3'}$, C$^{5,5'}$), 149.6 (C^d), 140.8 (C^c), 129.5 (*o*-C-OAr), 125.8 (*m*-C-OAr), 118.2 (*p*-C-OAr), 107.6 (C$^{4'}$), 107.3 (C^4),

78.3 (C^a), 69.4 (C^b), 41.4 (C^f), 40.9 (C^i), 39.9 (C^g, C^e), 31.4 (C^h), 26.7 (Me^k), 21.6 (Me^j), 17.5 ($\underline{CH_3}$-OAr), 13.3 (Me^3), 13.2 ($Me^{3'}$), 13.1 (Zn-$CH_2\underline{CH_3}$), 13.0 (Zn-$CH_2\underline{CH_3}$), 11.5 ($Me^{5'}$), 11.0 (Me^5), –3.1 (Zn-$\underline{CH_2}CH_3$), –5.9 (Zn-$\underline{CH_2}CH_3$). Elemental analysis (%) calcd for $C_{33}H_{48}N_4O_2Zn_2$: C, 59.73; H, 7.29; N, 8.44. Found: C, 59.77; H, 7.32; N, 8.48. $[\alpha]_D^{22}$ = +29.3 (*c* 10^{-3} g/mL, toluene).

Synthesis of [($ZnCH_2SiMe_3$)$_2$(*R*,*R*-bpzmm)(OAr)] (6). The synthesis of **6** was carried out in an identical manner to **4**. Compound **6** was obtained as a white solid. [Zn(CH_2SiMe_3)(bpzmm)Zn(CH_2SiMe_3)$_2$] (1.0 g, 1.34 mmol), 2,6-dimethylphenol (0.16 g, 1.34 mmol). Yield: 0.87 g (83%). ^{1}H NMR (C_6D_6, 297 K), δ 7.21 (d, 2H, $^3J_{H\text{-}H}$ = 7.1 Hz, *m*-H-OAr), 6.83 (t, 1H, $^3J_{H\text{-}H}$ = 7.1 Hz, *p*-H-OAr), 5.54 (bs, 2H, CH^b, CH^a), 5.38 (s, 1H, $H^{4'}$), 5.31 (s, 1H, H^4), 5.18 (bs, 1H, H^d), 2.38 (bs, 6H, $\underline{CH_3}$-OAr), 2.35–2.30 (m, 4H, $H^{e,f,i}$), 2.09 (s, 3H, $Me^{3'}$), 1.93 (s, 3H, Me^3), 1.84 (bs, 1H, H^h), 1.67 (s, 3H, $Me^{5'}$), 1.31 (s, 3H, Me^5), 1.29 (s, 3H, Me^j), 1.20 (d, 1H, $^2J_{H\text{-}H}$ = 8.4 Hz, H^h), 0.98 (s, 3H, Me^k), 0.32 (bs, 9H, Zn-$CH_2\underline{SiMe_3}$), 0.25 (bs, 9H, Zn-$CH_2\underline{SiMe_3}$), –0.40 (d, 1H, $^2J_{H\text{-}H}$ = 12.3 Hz, Zn-$\underline{CH_2}SiMe_3$), –0.59 (d, 1H, $^2J_{H\text{-}H}$ = 12.3 Hz, Zn-$\underline{CH_2}SiMe_3$), –0.62 (d, 1H, $^2J_{H\text{-}H}$ = 12.3 Hz, Zn-$\underline{CH_2}SiMe_3$), –0.71 (d, 1H, $^2J_{H\text{-}H}$ = 12.3 Hz, Zn-$\underline{CH_2}SiMe_3$). ^{13}C {^{1}H} NMR (C_6D_6, 297 K), δ 161.9 (C_{ipso}-OAr), 152.2–135.3 ($C^{3,3'}$, $C^{5,5'}$), 149.2 (C^d), 141.2 (C^c), 130.1 (*o*-C-OAr), 126.2 (*m*-C-OAr), 117.9 (*p*-C-OAr), 108.1 ($C^{4'}$), 107.6 (C^4), 77.6 (C^a), 69.9 (C^b), 40.8 (C^f), 40.6 (C^i), 39.9 (C^g, C^e), 31.2 (C^h), 26.1 (Me^k), 20.0 (Me^j), 19.5 ($\underline{CH_3}$-OAr), 13.5 (Me^3), 13.2 ($Me^{3'}$), 11.9 ($Me^{5'}$), 11.0 (Me^5), 1.9 (Zn-$CH_2\underline{SiMe_3}$), 1.3 (Zn-$CH_2\underline{SiMe_3}$), –6.2 (Zn-$\underline{CH_2}SiMe_3$), –7.1 (Zn-$\underline{CH_2}SiMe_3$). Elemental analysis (%) calcd for $C_{37}H_{60}N_4O_2Si_2Zn_2$: C, 56.98; H, 7.75; N, 7.18. Found: C, 57.02; H, 7.78; N, 7.15. $[\alpha]_D^{22}$ = +35.4 (*c* 10^{-3} g/mL, toluene).

Synthesis of [($ZnMe$)$_2$(*R*,*R*-bpzmm)(SAr)] (7). In a 250 cm^3 Schlenk tube, [Zn(Me)(bpzmm)Zn(Me_2)] (1.0 g, 1.89 mmol) was dissolved in dry toluene (60 mL) and the solution was cooled to –70 ºC. In other 100 mL Schlenk tube, 2,6-dimethylthiophenol (0.26 g, 1.89 mmol) was dissolved in dry toluene (20 mL) and precooled to –20 ºC. The solution of 2,6-dimethylthiophenol was added to the [Zn(Me)(bpzmm)Zn(Me_2)] solution dropwise and the mixture was allowed to warm up to room temperature and stirred during 20 min. The solvent was evaporated

to dryness under reduced pressure to yield a pale yellow solid, which was washed with cold *n*-hexane to give compound **7** as white solid. Yield: 1.10 g (89%). ^{1}H NMR (C_6D_6, 297 K), 7.00 (d, 2H, $^{3}J_{H\text{-}H}$ = 7.2 Hz, *m*-H-SAr), 6.88 (t, 1H, $^{3}J_{H\text{-}H}$ = 7.2 Hz, *p*-H-SAr), 5.59 (bs, 1H, CH^{b}), 5.54 (bs, 1H, CH^{a}), 5.34 (s, 1H, $H^{4'}$), 5.25 (s, 1H, H^{4}), 4.83 (bs, 1H, H^{d}), 2.76 (bs, 6H, $\underline{CH_3}$-SAr), 2.30–2.20 (m, 4H, $H^{e,f,i}$), 2.09 (s, 3H, $Me^{3'}$), 1.97 (s, 3H, Me^{3}), 1.84 (d, 1H, $^{2}J_{H\text{-}H}$ = 8.4 Hz, H^{h}), 1.58 (s, 6H, $Me^{5',5}$), 1.22 (s, 3H, Me^{j}), 0.98 (d, 1H, $^{2}J_{H\text{-}H}$ = 8.4 Hz, H^{h}), 0.88 (s, 3H, Me^{k}), –0.07 (bs, 6H, Zn-$\underline{CH_3}$), ^{13}C {^{1}H} NMR (C_6D_6, 297 K), δ 152.0–139.8 ($C^{3,3'}$, $C^{5,5'}$), 149.0 (C^{d}), 141.6 (C_{ipso}-SAr), 141.4 (C^{c}), 132.9 (*o*-C-SAr), 127.6 (*m*-C-SAr), 124.9 (*p*-C-SAr), 107.2 ($C^{4'}$), 106.4 (C^{4}), 78.7 (C^{a}), 69.3 (C^{b}), 41.9 (C^{f}), 41.3 (C^{i}), 38.1 (C^{g}, C^{e}), 32.2 (C^{h}), 27.1 (Me^{k}), 22.3 (Me^{j}), 17.0 ($\underline{CH_3}$-SAr), 13.6 (Me^{3}), 13.5 ($Me^{3'}$), 11.5 ($Me^{5'}$), 11.2 (Me^{5}), –14.5 (Zn-$\underline{Me}$), –14.9 (Zn-$\underline{Me}$). Elemental analysis (%) calcd for $C_{31}H_{44}N_4OSZn_2$: C, 57.14; H, 6.81; N, 8.60. Found: C, 57.12; H, 6.83; N, 8.66. $[\alpha]_D^{22}$ = +31.6 (*c* 10^{-3} g/mL, toluene).

Synthesis of [(ZnEt)$_2$(*R*,*R*-bpzmm)(SAr)] (8). The synthesis of **8** was carried out in an identical manner to **7**. Compound **8** was obtained as white solid. [Zn(Et)(bpzmm)Zn(Et)$_2$] (1.0 g, 1.75 mmol), 2,6-dimethylthiophenol (0.24 g, 1.75 mmol). Yield: 1.02 g (86%). ^{1}H NMR (C_6D_6, 297 K), δ 7.05 (d, 2H, $^{3}J_{H\text{-}H}$ = 7.2 Hz, *m*-H-SAr), 6.93 (t, 1H, $^{3}J_{H\text{-}H}$ = 7.2 Hz, *p*-H-SAr), 5.60 (bs, 2H, CH^{b}, CH^{a}), 5.36 (s, 1H, H^{4}), 5.34 (s, 1H, $H^{4'}$), 4.92 (bs, 1H, H^{d}), 2.78 (bs, 6H, $\underline{CH_3}$-SAr), 2.30–2.25 (m, 4H, $H^{e,f,i}$), 2.08 (s, 3H, $Me^{3'}$), 2.02 (s, 3H, Me^{3}), 1.97 (bs, 1H, H^{h}), 1.86 (bs, 3H, Zn-$CH_2\underline{CH_3}$), 1.85 (s, 3H, $Me^{5'}$), 1.62 (s, 3H, Me^{5}), 1.48 (bs, 3H, Zn-$CH_2\underline{CH_3}$), 1.27 (s, 3H, Me^{j}), 1.00 (d, 1H, $^{2}J_{H\text{-}H}$ = 8.4 Hz, H^{h}), 0.98 (s, 3H, Me^{k}), 0.65 (bs, 3H, Zn-$\underline{CH_2}CH_3$), 0.46 (bs, 3H, Zn-$\underline{CH_2}CH_3$). ^{13}C {^{1}H} NMR (C_6D_6, 297 K), δ 151.6–139.9 ($C^{3,3'}$, $C^{5,5'}$), 149.6 (C^{d}), 141.3 (C_{ipso}-SAr), 140.8 (C^{c}), 132.1 (*o*-C-SAr), 127.8 (*m*-C-SAr), 124.3 (*p*-C-SAr), 107.2 ($C^{4'}$), 106.9 (C^{4}), 78.3 (C^{a}), 69.3 (C^{b}), 41.9 (C^{f}), 40.3 (C^{i}), 39.1 (C^{g}, C^{e}), 31.9 (C^{h}), 26.9 (Me^{k}), 22.5 (Me^{j}), 16.5 ($\underline{CH_3}$-SAr), 13.1 ($Me^{3,3'}$), 13.0 (Zn-$CH_2\underline{CH_3}$), 12.8 (Zn-$CH_2\underline{CH_3}$), 11.6 ($Me^{5'}$), 10.9 (Me^{5}), –3.1 (Zn-$\underline{CH_2}CH_3$), –5.9 (Zn-$\underline{CH_2}CH_3$). Elemental analysis (%) calcd for $C_{33}H_{48}N_4OSZn_2$: C, 58.32; H, 7.12; N, 8.24. Found: C, 58.22; H, 7.16; N, 8.30. $[\alpha]_D^{22}$ = +29.3 (*c* 10^{-3} g/mL, toluene).

Synthesis of [($ZnCH_2SiMe_3)_2$(*R*,*R*-bpzmm)(SAr)] (9). The synthesis of **9** was carried out in an identical manner to **7**. Compound **9** was obtained as white solid. [$Zn(CH_2SiMe_3)$(bpzmm)$Zn(CH_2SiMe_3)_2$] (1.0 g, 1.34 mmol), 2,6-dimethylthiophenol (0.19 g, 1.34 mmol). Yield: 0.91 g (85%). ^{1}H NMR (C_6D_6, 297 K), δ 7.10 (d, 2H, $^3J_{H\text{-}H}$ = 7.2 Hz, *m*-H-SAr), 6.98 (t, 1H, $^3J_{H\text{-}H}$ = 7.2 Hz, *p*-H-SAr), 5.44 (bs, 2H, CH^b, CH^a), 5.29 (s, 1H, $H^{4'}$), 5.26 (s, 1H, H^4), 4.93 (bs, 1H, H^d), 2.71 (bs, 6H, $\underline{CH_3}$-SAr), 2.45–2.30 (m, 4H, $H^{e,f,i}$), 2.11 (s, 3H, $Me^{3'}$), 1.99 (s, 3H, Me^3), 1.92 (bs, 1H, H^h), 1.55 (s, 3H, $Me^{5'}$), 1.41 (s, 3H, Me^5), 1.33 (s, 3H, Me^j), 1.21 (d, 1H, $^2J_{H\text{-}H}$ = 8.4 Hz, H^h), 1.03 (s, 3H, Me^k), 0.26 (bs, 9H, Zn-$CH_2\underline{SiMe_3}$), 0.20 (bs, 9H, Zn-CH_2-$\underline{SiMe_3}$), –0.45 (d, 1H, $^2J_{H\text{-}H}$ = 12.3 Hz, Zn-$\underline{CH_2}SiMe_3$), –0.63 (d, 1H, $^2J_{H\text{-}H}$ = 12.3 Hz, Zn-$\underline{CH_2}SiMe_3$), –0.72 (d, 1H, $^2J_{H\text{-}H}$ = 12.3 Hz, Zn-$\underline{CH_2}SiMe_3$), –0.79 (d, 1H, $^2J_{H\text{-}H}$ = 12.3 Hz, Zn-$\underline{CH_2}SiMe_3$). ^{13}C {^{1}H} NMR (C_6D_6, 297 K), δ 150.9–133.1 ($Me^{3,3'}$, $Me^{5,5'}$), 149.2 (C^d), 141.9 (C_{ipso}-SAr), 140.2 (C^c), 133.1 (*o*-C-SAr), 127.6 (*m*-C-SAr), 122.9 (*p*-C-SAr), 108.1 ($C^{4'}$), 106.2 (C^4), 75.6 (C^a), 68.5 (C^b), 42.0 (C^f), 41.6 (C^i), 39.1 (C^g, C^e), 31.2 (C^h), 26.9 (Me^k), 21.0 (Me^j), 16.5 ($\underline{CH_3}$-SAr), 13.3 (Me^3), 13.1 ($Me^{3'}$), 12.3 ($Me^{5'}$), 11.4 (Me^5), 0.9 (Zn-$CH_2\underline{SiMe_3}$), 0.6 (Zn-$CH_2\underline{SiMe_3}$), –7.8 (Zn-$\underline{CH_2}SiMe_3$), –8.3 (Zn-$\underline{CH_2}SiMe_3$). Elemental analysis (%) calcd for $C_{37}H_{60}N_4OSSi_2Zn_2$: C, 55.83; H, 7.60; N, 7.04. Found: C, 55.84; H, 7.67; N, 7.00. $[\alpha]_D^{22}$ = +31.1 (*c* 10^{-3} g/mL, toluene).

General Polymerization Procedures. Polymerizations of L-lactide and *rac*-lactide (LA) were performed on a Schlenk line in a flame-dried round-bottomed flask equipped with a magnetic stirrer. The Schlenk tubes were charged in the glovebox with the required amount of lactide and initiator, separately, and then attached to the vacuum line. The initiator and monomer were dissolved in the appropriate amount of solvent, and temperature equilibration was ensured in both Schlenk flasks by stirring the solutions for 15 min in a bath. The appropriate amount of initiator was added by syringe, and polymerization times were measured from that point. Polymerizations were stopped by injecting a solution of hydrochloric acid in methanol. Polymers were precipitated in methanol, filtered off, redissolved and reprecipitated in methanol and finally dried in vacuo to constant weight.

Typical Kinetic Procedure. A solution of catalyst in tetrahydrofuran (2.5 mL) was added to a solution of monomer (10 mL) in the same solvent, to give a $[\text{L-LA}]_0$ = 0.72 M. The initial ratio monomer/catalyst was $[\text{L-LA}]_0/[\text{catalyst}]_0$ = 90 and the initial catalyst $[\text{catalyst}]_0$ = 8 mM was modified up to 20 mM. The resulting mixture was stirred at 50ºC under an N_2 atmosphere. At appropriate time intervals, 0.5 mL aliquots were removed using a syringe and quickly quenched into 5 mL vials with wet methanol (3 drops). The aliquots were then dried to constant weight in vacuo and analyzed by ^{1}H NMR spectroscopy. The standard error associated with the kinetic parameters was calculated by the standard deviation in slope and intercept for each regression analysis.

X-ray Structure Determination: X-ray data of **2**, and **5** were collected with Bruker X8 APEX II CCD area detector diffractometer at T = 230 K using graphite monochromated Mo-Kα radiation (λ = 0.71073 Å, sealed X-ray tube). Data were integrated using SAINT[48] and an absorption correction was performed with the program SADABS.[49] The structures were solved by direct methods using SHELXTL,[50] and refined by full-matrix least-squares methods based on F^2. Non-hydrogen atoms were refined anisotropically. All of the hydrogen atoms were placed in calculated positions and thereafter treated as riding. Salient crystallographic data are summarized in Table S3. Selected geometric data are presented in Table 1.

Acknowledgments. We gratefully acknowledge financial support from the Ministerio de Economía y Competitiviadad (MINECO), Spain (Grant No. CTQ2011-22578/BQU and Consolider-Ingenio 2010 ORFEO CSD2007-00006).

Supporting Information Available. Ring-opening polymerization of L- and *rac*-lactide details and X-ray diffraction experimental details of data collection, refinement, atom coordinates as well as anisotropic displacement parameters for complexes **2** and **5**. This material is available free of charge via the Internet at http://pubs.acs.org.

References

(1) (a) Pego, A. P.; Siebum, B.; Van Luyn, M. J.; Gallego y Van Seijen, X. J.; Poot, A. A.; Grijpma, D. W.; Feijen, J. *Tissue Eng.* **2003**, *9*, 981-94. (b) Vacanti, J. P.; Langer, R.; Upton, J.; Marler, J. J. *Adv Drug Deliv Rev.* **1998**, *33*, 165-182. (c) Frazza, E. J.; Schmitt, E. E. *Journal of Biomedical Materials Research* **1971**, *5*, 43-58. (d) Dexon and Vicryl are products of Davis & Geek Corp., Wayne, NJ, and Ethicon, Inc., Somerville, NJ, respectively.

(2) (a) Penco, M.; Donetti, R.; Mendichi, R.; Ferruti, P. *Macromol. Chem. Phys.* **1998**, *199*, 1737-1745. (b) Leupron Depot is a product of Takeda Chemical Industries, Ltd., Japan, for drug delivery purposes. (c) Kim, H.; Sung, Y. K.; Jung, J.; Baik, H.; Min, T. J.; Kim, Y. S. *J. Korean Chem. Soc.* **1990**, *34*, 8. (d) Smith, A.; Hunneyball, l. M. *Int. J. Pharm.* **1986**, *30*, 215-220.

(3) (a) Darensbourg, D. J.; Choi, W.; Richers, C. P. *Macromolecules* **2007**, *40*, 3521-3523. (b) Beiser, I. H.; Kanat, I. O. *J Am Podiatr Med Assoc* **1990**, *80*, 72-5.

(4) For reviews in this area see: (a) Otero, A.; Fernández-Baeza, J.; Lara-Sánchez, A.; Sánchez-Barba, L. F. *Coord. Chem. Rev.* **2013**, *257*, 1806-1868. (b) Cameron, D. J. A.; Shaver, M. P. *Chem. Soc. Rev.* **2011**, *40*, 1761-1776. (c) Kiesewetter, M. K.; Shin, E. J.; Hedrick, J. L.; Waymouth, R. M. *Macromolecules* **2010**, *43*, 2093-2107. (d) Stanford, M. J.; Dove, A. P. *Chem. Soc. Rev.* **2010**, *39*, 486-494. (e) Carpentier, J.-F. *Macromol. Rapid Commun.* **2010**, *31*, 1696-1705. (f) Thomas, C. M. *Chem. Soc. Rev.* **2010**, *39*, 165-173. (g) Ajellal, N.; Carpentier, J.-F.; Guillaume, C.; Guillaume, S. M.; Helou, M.; Poirier, V.; Sarazin, Y.; Trifonov, A. *Dalton Trans.* **2010**, *39*, 8363-8376. (h) Wheaton, C. A.; Hayes, P. G.; Ireland, B. J. *Dalton Trans.* **2009**, 4832-4846. (i) Place, E. S.; George, J. H.; Williams, C. K.; Stevens, M. M. *Chem. Soc. Rev.* **2009**, *38*, 1139-1151. (j) Platel, R. H.; Hodgson, L. M.; Williams, C. K. *Polymer Reviews* **2008**, *48*, 11-63. (k) Williams, C. K.; Hillmyer, M. A. *Polymer Reviews* **2008**, *48*, 1-10. (l) Dove, A. P. *Chem. Commun.* **2008**, 6446-6470. (m) Amgoune, A.; Thomas, C. M.; Roisnel, T.; Carpentier, J.-F. *Chem. –Eur. J.* **2006**, *12*, 169-179. (n) Wu, J.; Yu, T.-L.; Chen, C.-T.; Lin, C.-C. *Coord. Chem. Rev.* **2006**, *250*, 602-626. (o) Dechy-

Cabaret, O.; Martin-Vaca, B.; Bourissou, D. *Chem. Rev.* **2004**, *104*, 6147-6176. (p) Chisholm, M. H.; Zhou, Z. *J. Mater. Chem.* **2004**, *14*, 3081-3092.

(5) (a) Auras, R.; Lim, L.-T., *Poly(lactic acid) : synthesis,* structures*, properties, processing, and applications*. Wiley: Hoboken, NJ, **2010**. (b) Dubois, P.; Coulembier, O.; Raquez, J.-M., *Handbook of ring-opening polymerization*. Wiley-VCH: Weinheim, **2009**. (c) Chisholm, M. H.; Zhou, Z., Stereoselective polymerization of Lactide. In *Stereoselective Polymerization with Single Site Catalysts*, Baugh, L. S.; Canich, J. A. M., Eds. CRC Press, Taylor & Francis: Boca Raton, Florida, **2008**; pp 645-660.

(6) (a) Biela, T.; Kowalski, A.; Libiszowski, J.; Duda, A.; Penczek, S. *Macromolecular Symposia* **2006**, *240*, 47-55. (b) Ragauskas, A. J.; Williams, C. K.; Davison, B. H.; Britovsek, G.; Cairney, J.; Eckert, C. A.; Frederick, W. J., Jr.; Hallett, J. P.; Leak, D. J.; Liotta, C. L.; Mielenz, J. R.; Murphy, R.; Templer, R.; Tschaplinski, T. *Science* **2006**, *311*, 484-9.

(7) (a) Buffet, J.-C.; Okuda, J. *Polym. Chem.* **2011**, *2*, 2758-2763. (b) Shaver, M. P.; Cameron, D. J. A. *Biomacromolecules* **2010**, *11*, 3673-3679.

(8) Nomura, N.; Ishii, R.; Yamamoto, Y.; Kondo, T. *Chem.* –Eur. *J.* **2007**, *13*, 4433-4451.

(9) Nomura, N.; Ishii, R.; Akakura, M.; Aoi, K. *J.* Am. *Chem. Soc.* **2002**, *124*, 5938-5939.

(10) Sánchez-Barba, L. F.; Garcés, A.; Fajardo, M.; Alonso-Moreno, C.; Fernández-Baeza, J.; Otero, A.; Antiñolo, A.; Tejeda, J.; Lara-Sánchez, A.; López-Solera, M. I. *Organometallics* **2007**, *26*, 6403-6411.

(11) Spinu, M.; Jackson, C.; Keating, M. Y.; Gardner, K. H. *Journal of Macromolecular Science, Part A* **1996**, *33*, 1497-1530.

(12) Sanchez-Barba, L. F.; Alonso-Moreno, C.; Garces, A.; Fajardo, M.; Fernandez-Baeza, J.; Otero, A.; Lara-Sanchez, A.; Rodriguez, A. M.; Lopez-Solera, I. *Dalton Trans.* **2009**, 8054-8062.

(13) (a) Garcés, A.; Sánchez-Barba, L. F.; Alonso-Moreno, C.; Fajardo, M.; Fernández-Baeza, J.; Otero, A.; Lara-Sánchez, A.; López-Solera, I.; Rodríguez, A. M. *Inorg. Chem.* **2010**, *49*, 2859-2871. (b) Otero, A.; Fernandez-Baeza, J.; Lara-Sanchez, A.; Antiñolo, A.; Tejeda, J.; Martinez-Caballero, E.; Marquez-Segovia, I.; Lopez-Solera, I.; Sanchez-Barba, L. F.; Alonso-Moreno, C. *Inorg Chem* **2008**, *47*, 4996-5005. (c) Otero, A.; Fernández-Baeza, J.; Antiñolo, A.; Tejeda, J.; Lara-Sánchez, A.; Sánchez-Barba, L. F.; Sánchez-Molina, M.; Rodríguez, A. M.; Bo, C.; Urbano-Cuadrado, M. *Organometallics* **2007**, *26*, 4310-4320.

(14) (a) Chamberlain, B. M.; Cheng, M.; Moore, D. R.; Ovitt, T. M.; Lobkovsky, E. B.; Coates, G. W. *J. Am. Chem. Soc.* **2001**, *123*, 3229-3238. (b) Chisholm, M. H.; Eilerts, N. W.; Huffman, J. C.; Iyer, S. S.; Pacold, M.; Phomphrai, K. *J. Am. Chem. Soc.* **2000**, *122*, 11845-11854. (c) Ovitt, T. M.; Coates, G. W. *J. Am. Chem. Soc.* **1999**, *121*, 4072-4073.

(15) Alonso-Moreno, C.; Garcés, A.; Sánchez-Barba, L. F.; Fajardo, M.; Fernández-Baeza, J.; Otero, A.; Lara-Sánchez, A.; Antiñolo, A.; Broomfield, L.; López-Solera, M. I.; Rodríguez, A. M. *Organometallics* **2008**, *27*, 1310-1321.

(16) Sánchez-Barba, L. F.; Garcés, A.; Fernández-Baeza, J.; Otero, A.; Alonso-Moreno, C.; Lara-Sánchez, A.; Rodríguez, A. M. *Organometallics* **2011**, *30*, 2775-2789.

(17) (a) Garcés, A.; Sánchez-Barba, L. F.; Fernández-Baeza, J.; Otero, A.; Honrado, M.; Lara-Sánchez, A.; Rodríguez, A. M. *Inorg. Chem*. **2013**, *52*, 12691-12701. (b) Xie, H.; Mou, Z.; Liu, B.; Li, P.; Rong, W.; Li, S.; Cui, D. M. *Organometallics*, **2014**, *33*, 722–730.

(18) (a) Stopper, A.; Okuda, J.; Kol, M. *Macromolecules* **2012**, *45*, 698-704. (b) Du, H.; Velders, A. H.; Dijkstra, P. J.; Zhong, Z.; Chen, X.; Feijen, J. *Macromolecules* **2009**, *42*, 1058-1066. (c) Alaaeddine, A.; Thomas, C. M.; Roisnel, T.; Carpentier, J.-F. *Organometallics* **2009**, *28*, 1469-1475. (d) Jhurry, D.; Bhaw-Luximon, A.; Spassky, N. *Macromolecular Symposia* **2001**, *175*, 67-80.

(19) (a) Bakewell, C.; Platel, R. H.; Cary, S. K.; Hubbard, S. M.; Roaf, J. M.; Levine, A. C.; White, A. J. P.; Long, N. J.; Haaf, M.; Williams, C. K. *Organometallics* **2012**, *31*, 4729-4736. (b) Chen, H.-

L.; Dutta, S.; Huang, P.-Y.; Lin, C.-C. *Organometallics* **2012**, *31*, 2016-2025. (c) Matsubara, K.; Terata, C.; Sekine, H.; Yamatani, K.; Harada, T.; Eda, K.; Dan, M.; Koga, Y.; Yasuniwa, M. *J. Polym. Sci., Part A: Polym. Chem.* **2012**, *50*, 957-966. (d) Bouyahyi, M.; Roisnel, T.; Carpentier, J.-F. *Organometallics* **2012**, *31*, 1458-1466. (e) Normand, M.; Kirillov, E.; Roisnel, T.; Carpentier, J.-F. *Organometallics* **2012**, *31*, 1448-1457. (f) Zhong, Z.; Dijkstra, P. J.; Feijen, J. *Angew. Chem. Int. Ed.* **2002**, *41*, 4510-4513.

(20) Douglas, A. F.; Patrick, B. O.; Mehrkhodavandi, P. *Angew. Chem. Int. Ed.* **2008**, *47*, 2290-2293.

(21) (a) Arnold, P. L.; Buffet, J.-C.; Blaudeck, R.; Sujecki, S.; Wilson, C. *Chem. –Eur. J.* **2009**, *15*, 8241-8250. (b) Arnold, P. L.; Buffet, J.-C.; Blaudeck, R. P.; Sujecki, S.; Blake, A. J.; Wilson, C., *Angew. Chem. Int. Ed.* **2008**, *47*, 6033-6036.

(22) Otero, A.; Fernández-Baeza, J.; Lara-Sánchez, A.; Alonso-Moreno, C.; Márquez-Segovia, I.; Sánchez-Barba, L. F.; Rodríguez, A. M. *Angew. Chem. Int. Ed.* **2009**, *48*, 2176-2179.

(23) (a) Parkin, G. *Chem. Commun.* **2000**, 1971-1985. (b) Mills, C. F., *Zinc in human biology*. Springer-Verlag: London, 1989.

(24) (a) Gao, B.; Duan, R.; Pang, X. Li, X.; Qu, Z.; Shao, H.; Wang, X.; Chen, X. *Dalton Trans.* **2013**, *42*, 16334-16342. (b) Yu, X.-F.; Zhang, C.; Wang, Z.-X. *Organometallics*, **2013**, *32*, 3262-3268. (c) Wang, Y.; Zhao, W.; Liu, D.; Li, S.; Liu, X.; Cui, D.; Chen, X. *Organometallics* **2012**, *31*, 4182-4190. (d) Piedra-Arroni, E.; Brignou, P.; Amgoune, A.; Guillaume, S. M.; Carpentier, J.-F.; Bourissou, D. *Chem. Commun.* **2011**, *47*, 9828-9830. (e) Chisholm, M. H. *Pure Appl. Chem.* **2010**, *82*. (f) Drouin, F.; Oguadinma, P. O.; Whitehorne, T. J. J.; Prud'homme, R. E.; Schaper, F. *Organometallics* **2010**, *29*, 2139-2147. (g) Schofield, A. D.; Barros, M. L.; Cushion, M. G.; Schwarz, A. D.; Mountford, P. *Dalton Trans.* **2009**, 85-96. (h) Otero, A.; Fernández-Baeza, J.; Antiñolo, A.; Tejeda, J.; Lara-Sánchez, A.; Sánchez-Barba, L.; Rodríguez, Ana M. *Eur. J. Inorg. Chem.* **2004**, 260-266. (i) Williams, C. K.; Breyfogle, L. E.; Choi, S. K.; Nam, W.; Young, V. G.;

Hillmyer, M. A.; Tolman, W. B. *J. Am. Chem. Soc.* **2003**, *125*, 11350-11359. (j) Cheng, M.; Attygalle, A. B.; Lobkovsky, E. B.; Coates, G. W. *J. Am. Chem. Soc.* **1999**, *121*, 11583-11584. (k) Several zinc initiators have been reported to promote isoactivity in the ROP of *rac*-LA through a chain end control mechanism. See for example: Song, S.; Zhang, X.; Ma, H.; Yang, Y. *Dalton Trans.* **2012**, *41*, 3266-3277.

(25) Chakraborty, D.; Chen, E. Y. X. *Organometallics* **2003**, *22*, 769-774.

(26) Wu, J.-C.; Huang, B.-H.; Hsueh, M.-L.; Lai, S.-L.; Lin, C.-C. *Polymer* **2005**, *46*, 9784-9792.

(27) (a) Farwell, J. D.; Hitchcock, P. B.; Lappert, M. F.; Luinstra, G. A.; Protchenko, A. V.; Wei, X.-H. *J. Organomet. Chem.* **2008**, *693*, 1861-1869. (b) Darensbourg, D. J.; Karroonnirun, O. *Inorg. Chem.* **2010**, *49*, 2360-2371. (c) Darensbourg, D. J.; Karroonnirun, O. *Macromolecules* **2010**, *43*, 8880-8886.

(28) Honrado, M.; Otero, A.; Fernández-Baeza, J.; Sánchez-Barba, L. F.; Lara-Sánchez, A.; Tejeda, J.; Carrión, M. P.; Martínez-Ferrer, J.; Garcés, A.; Rodríguez, A. M. *Organometallics* **2013**, *32*, 3437–3440.

(29) Wang, H.; Ma, H. *Chem. Commun.* **2013**, *49*, 8686-8688.

(30) Otero, A.; Fernández-Baeza, J.; Lara-Sánchez, A.; Tejeda, J.; Sánchez-Barba, L. F. *Eur. J. Inorg. Chem.* **2008**, *2008*, 5309-5326.

(31) (a) Otero, A.; Fernández-Baeza, J.; Tejeda, J.; Lara-Sánchez, A.; Sánchez-Molina, M.; Franco, S.; López-Solera, I.; Rodríguez, A. M.; Sánchez-Barba, L. F.; Morante-Zarcero, S.; Garcés, A. *Inorg. Chem.* **2009**, *48*, 5540-5554. (b) Otero, A.; Fernández-Baeza, J.; Antiñolo, A.; Tejeda, J.; Lara-Sánchez, A.; Sánchez-Barba, L. F.; Sánchez-Molina, M.; Franco, S.; López-Solera, M. I.; Rodríguez, A. M. *Inorg. Chem.* **2007**, *46*, 8475-8477. (c) Otero, A.; Fernandez-Baeza, J.; Antiñolo, A.; Tejeda, J.; Lara-Sanchez, A.; Sanchez-Barba, L.; Exposito, M. T.; Rodriguez, A. M. *Dalton Trans.* **2003**, 1614-1619.

(32) Otero, A.; Fernández-Baeza, J.; Sánchez-Barba, L. F.; Tejeda, J.; Honrado, M.; Garcés, A.; Lara-Sánchez, A.; Rodríguez, A. M. *Organometallics* **2012**, *31*, 4191-4202.

(33) Neu, R. C.; Otten, E.; Stephan D. W. *Angew. Chem., Int. Ed.* **2009**, 9709-9712.

(34) Boyle, T. J.; Pratt, H. D.; Alam, T. M.; Headley, T.; Rodriguez, M. A. *Eur. J. Inorg. Chem.* **2009**, 855-865.

(35) Grunova, E.; Roisnel, T.; Carpentier, J.-F. *Dalton Trans.* **2009**, 9010-9019.

(36) Poirier, V.; Roisnel, T.; Carpentier, J.-F.; Sarazin, Y. *Dalton Trans.* **2009**, 9820-9827.

(37) Johnson, A. L.; Hollingsworth, N.; Kociok-Köhn, G.; Molloy, K. C. *Inorg. Chem.* **2008**, *47*, 12040-12048.

(38) (a) Becker, J. M.; Pounder, R. J.; Dove, A. P. *Macromol. Rapid Commun.* **2010**, *31*, 1923-1937. (b) Zhong, Z.; Dijkstra, P. J.; Feijen, J. *J. Am. Chem. Soc.* **2003**, *125*, 11291-11298. (c) Radano, C. P.; Baker, G. L.; Smith, M. R. *J. Am. Chem. Soc.* **2000**, *122*, 1552-1553.

(39) Sarazin, Y.; Liu, B.; Roisnel, T.; Maron, L.; Carpentier, J.-F. *J. Am. Chem. Soc.* **2011**, *133*, 9069-9087.

(40) Poirier, V.; Roisnel, T.; Carpentier, J.-F.; Sarazin, Y. *Dalton Trans.* **2011**, *40*, 523-534.

(41) (a) Sánchez-Barba, L. F.; Hughes, D. L.; Humphrey, S. M.; Bochmann, M. *Organometallics* **2006**, *25*, 1012-1020. (b) Sánchez-Barba, L. F.; Hughes, D. L.; Humphrey, S. M.; Bochmann, M. *Organometallics* **2005**, *24*, 5329-5334.

(42) Börner, J.; dos Santos Vieira, I.; Pawlis, A.; Döring, A.; Kuckling, D.; Herres-Pawlis, S. *Chem. –Eur. J.* **2011**, *17*, 4507-4512.

(43) (a) Baran, J.; Duda, A.; Kowalski, A.; Szymanski, R.; Penczek, S. *Macromol. Rapid* Commun. **1997**, *18*, 325-333. (b) Barakat, I.; Dubois, P.; Jérôme, R.; Teyssié, P., *J. Polym. Sci., Part A: Polym. Chem.* **1993**, *31*, 505-514.

(44) Ovitt, T. M.; Coates, G. W. *J. Am. Chem. Soc.* **2002**, *124*, 1316-1326.

(45) Chisholm, M. H.; Huffman, J. C.; Phomphrai, K. *J. Chem. Soc., Dalton Trans.* **2001**, 222-224.

(46) Coudane, J.; Ustariz-Peyret, C.; Schwach, G.; Vert, M. *J. Polym. Sci., Part A: Polym. Chem.* **1997**, *35*, 1651-1658.

(47) Hartwell, G. E.; Brown, T. L. *Inorg. Chem.* **1966**, *5*, 1257-1259.

(48) SAINT+ v7.12a. Area-Detector Integration Program. Bruker-Nonius AXS. Madison, Wisconsin, USA, 2004.

(49) G. M. Sheldrick, SADABS version 2004/1. A Program for Empirical Absorption Correction. University of Göttingen, Göttingen, Germany, 2004.

(50) SHELXTL-NT version 6.12. Structure Determination Package. Bruker-Nonius AXS. Madison, Wisconsin, USA, 2001.

GRAPHIC TABLE OF CONTENTS ENTRY

Stereoselective ROP of *rac*-Lactide Mediated by Enantiopure NNO-Scorpionate Zinc Initiators.

Manuel Honrado,[†] Antonio Otero,[,†] Juan Fernández-Baeza,[*,†] Luis F. Sánchez-Barba,[*,‡] Andrés Garcés,[‡] Agustín Lara-Sánchez[†] and Ana M. Rodríguez[†]*

A sterically hindered and enantiopure alkyl-aryloxide-containing zinc heteroscorpionate represents one of the first examples of a zinc initiator capable of exerting significant levels of enantioselectivity in the growing polymer microstructure ($P_i = 0.74$), through an enantiomorphic site control mechanism.